Fine-structure splitting of exciton states in semiconductor quantum dot molecules

2008 J. Phys.: Condens. Matter 20 045204

(http://iopscience.iop.org/0953-8984/20/4/045204)

J. Phys.: Condens. Matter **20** (2008) 045204 (8pp) doi:10.1088/0953-8984/20/04/045204

Fine-structure splitting of exciton states in semiconductor quantum dot molecules

Dong Xu, Nan Zhao and Jia-Lin Zhu

Department of Physics, Tsinghua University, Beijing 100084, People's Republic of China

E-mail: zjl-dmp@tsinghua.edu.cn

Received 1 November 2007, in final form 10 December 2007
Published 8 January 2008
Online at stacks.iop.org/JPhysCM/20/045204

Abstract

Exciton levels and fine-structure splitting in laterally coupled quantum dot molecules are studied. The electron and hole tunnelling energies as well as the direct Coulomb interaction are essential for the exciton levels. It is found that fine-structure splittings of the two lowest exciton levels are contributed by the intra- and interdot exchange interactions which are greatly influenced by the symmetry and tunnel-coupling between the two dots. As the interdot separation is reduced, fine-structure splitting of the exciton ground state is largely increased while those of the second and fourth states are decreased. Moreover, the dependence of the fine-structure splitting in quantum dot molecules on the Coulomb correlation is clearly clarified.

(Some figures in this article are in colour only in the electronic version)

1. Introduction

During the last few years there has been intensive study of the optical properties of single semiconductor quantum dots (QDs), since they exhibit an atom-like energy spectrum and sharp lines in photoluminescence and can also be conveniently manipulated by external fields. Semiconductor QDs have been demonstrated as one possible candidate for single-photon or entangled two-photon sources, making them very attractive for applications in the fields of quantum cryptography and quantum teleportation [1–7]. In the first proposal for a QD-based source of polarization entangled photon pairs, a necessary condition was that the intermediate monoexciton states for the biexciton radiative decay are energetically degenerate [8]. However, III–V self-assembled semiconductor QDs tend to be elongated along the $[\bar{1}10]$ crystal axis and the monoexciton states are split by the anisotropic electron–hole exchange interaction [9–14]. Consequently, much effort has been devoted to reducing the fine-structure splitting of the intermediate exciton states, e.g. thermal annealing and external field tuning [15–21].

Neglecting the electron–hole exchange interaction, the exciton ground state is four-fold degenerate. For $In_xGa_{1-x}As$ QDs with C_{2v} or lower symmetry, however, the electron–hole exchange interaction splits the exciton ground state into bright and dark doublets, which are separated by about a few hundred μeV [22]. Furthermore, the bright doublets are split into two linearly polarized states separated by some tens of μeV [23]. At zero external field, the fine-structure splitting of the bright doublet mainly depends on the anisotropy and size of the QDs [12–14]. If a magnetic field is applied in a Voigt configuration, the bright states are mixed with the dark states through the Zeeman term and the dark exciton states become optically active [22, 23]. Due to the Zeeman splitting induced by the magnetic field, the fine-structure splitting of the bright doublet could be tuned to zero by the magnetic field [6, 19]. In addition, thermal annealing [15, 16] and an in-plane electric field [20, 21] could lead to a significant reduction of the fine-structure splitting.

Recently, with the development of high-quality QD structures, it has been possible to fabricate either vertically or laterally coupled self-assembled QDs, namely a 'quantum dot molecule' (QDM) [24–28]. The exciton ground states exhibit fine structures induced by the electron and hole tunnel-coupling between the two dots [29]. The exciton states and interdot coupling could be manipulated by the electric field in either a vertically or laterally coupled QDM [28, 30–35]. A significant Stark effect [28, 30] and pronounced anticrossing of different excitonic transitions [31] have been observed in the photoluminescence (PL) spectra. According to several numerical calculations [32, 35, 36], interdot coupling as well as the symmetry between the two dots strongly influence the exciton levels and optical properties.

Previously, we found that fine-structure splitting of the exciton ground state in a laterally coupled QDM could be tuned to zero by applying an in-plane electric field of only a few kV cm^{-1}, which might overcome the deficiency in a single QD [37]. Polarization entangled photon pairs might be prepared in a QDM through biexciton radiative decay. Thus, clarification of the mechanism of the variation of fine-structure splitting in QDMs with various interdot separations is very important. In this paper, we study the symmetry and tunnel-coupling effects on the fine-structure splitting of exciton states in QDMs. Exciton levels of symmetric and nonsymmetric QDMs without the electron–hole exchange interaction are given, and we note that the exciton level spacing is much larger than the electron–hole exchange energies. Fine-structure splittings of the two lowest exciton levels are contributed by the intra- and interdot exchange interactions. Symmetry and tunnel-coupling in QDMs strongly influence the exciton envelope functions, and therefore it is interesting that intra- and interdot exchange interactions might be strongly dependent on the symmetry and tunnel-coupling. Moreover, the variations of the fine-structure splittings of exciton ground and excited states are compared and discussed.

In section 2, a microscopic theory of exciton levels and fine-structure splitting in a QDM is formulated. In section 3, exciton levels in a QDM without the exchange interaction are given and discussed. Fine-structure splittings of a few low-lying bright exciton states are shown for both symmetric and nonsymmetric QDMs. The intra- and interdot parts of the splittings of the two lowest exciton levels are given and compared. The effects of the symmetry and tunnel-coupling as well as the Coulomb correlation are clearly clarified. Finally, the results are summarized in section 4.

2. Description of exciton levels and fine-structure splitting

The exciton fine-structure splitting in the semiconductor QDs is contributed from the electron–hole exchange interaction. Study of the electron–hole exchange interaction requires a clear representation of the spin states of the exciton. In a bulk III–V direct-gap semiconductor, the valence-band edge has Γ_8 symmetry ($J = 3/2$) and the conduction band edge has Γ_6 symmetry. For the flat InGaAs quantum dots investigated in this paper, the light- ($J_z = \pm 1/2$) and heavy-hole ($J_z = \pm 3/2$) bands are split by several tens of meV due to the strain introduced by the lattice mismatch. Actually, according to an empirical tight-binding calculation [38], the proportion of heavy-hole component in the hole ground state of a flat InGaAs QD is as large as 98.2%. Therefore, it is reasonable that the light-hole and spin–orbit-split $J = 1/2$ valence band can be neglected since we mainly focus on the fine-structure splittings of a few low-lying exciton states. The exciton state is composed of four combinations of the valence band and the conduction band, i.e.

$$|X\rangle = \sum_{m,s}\sum_{r_e,r_h} \psi_{ms}(r_e, r_h) a^{\dagger}_{c_s r_e} a_{v_m r_h}|0\rangle, \tag{1}$$

where the Wannier function representation of the creation and annihilation operators is used, m and s are the z component of the angular momentum of the heavy-hole valence band and the conduction band, respectively, and $\psi_{ms}(r_e, r_h)$ is the envelope function with $r_{e(h)}$ the position vector of the electron (hole). The z component of the exciton spin for state (m, s) is $s - m$. From the selection rule, the spin ± 1 exciton states might be optically active depending on the orbital envelope functions, while the spin ± 2 states are optically inactive, irrespective of the orbital envelope functions. The eigenvalue equation for ψ_{ms} is given as

$$\sum_{m's'r'_e r'_h} [H_1 + V_{ex}(c_s r_e, v_{m'} r'_h; c_{s'} r'_e, v_m r_h)] \times \psi_{m's'}(r'_e, r'_h) = E\psi_{ms}(r_e, r_h), \tag{2}$$

with the spin-independent part

$$H_1 = \delta_{r_e r'_e}\delta_{r_h r'_h}\delta_{s's}\delta_{m'm}\left[\frac{p_e^2}{2m_e} + U_e(r_e) + \frac{p_h^2}{2m_h} + U_h(r_h) - \frac{e^2}{\epsilon|r_e - r_h|}\right], \tag{3}$$

where U_e (U_h) is the confinement potential for the conduction (valence) band electron. The electron–hole exchange interaction V_{ex} can be approximated as

$$\begin{aligned} &V_{ex}(c_s r_e, v_{m'} r'_h; c_{s'} r'_e, v_m r_h) \\ &\approx \delta_{r_e r_h}\delta_{r'_e r'_h}\left[\delta_{r_e r'_e} V(c_s r_e, v_{m'} r_e; c_{s'} r_e, v_m r_e) \right. \\ &\quad \left. + (1 - \delta_{r_e r'_e}) V(c_s r_e, v_{m'} r'_e; c_{s'} r'_e, v_m r_e)\right]. \end{aligned} \tag{4}$$

The first (second) term of equation (4) is the so-called short-range (long-range) exchange interaction. The long-range term can be further approximated through the multipole expansion

$$V(c_s r_e, v_{m'} r'_e; c_{s'} r'_e, v_m r_e) \approx \vec{\mu}_{c_s, v_m} \frac{[1 - 3n \cdot^t n]}{|r_e - r'_e|^3} \vec{\mu}_{v_{m'}, c_{s'}} \tag{5}$$

with

$$\begin{aligned} n &= \frac{r_e - r'_e}{|r_e - r'_e|}, \\ \vec{\mu}_{c_s, v_m} &= e\int \mathrm{d}^3 r \phi^*_{c_s R}(r)(r - R)\phi_{v_m R}(r) \end{aligned} \tag{6}$$

where $\phi_{cs(vm)R}(r)$ is a Wannier function localized at the site R. The matrix element of V_{ex} is given as [13]

$$\begin{aligned} V_{anal}(ms, m's') &\int \mathrm{d}^3 r \psi^*_{ms}(r, r)\psi_{m's'}(r, r) \\ &+ \int \mathrm{d}^3 r \ \mathrm{div}_r(\psi^*_{ms}(r, r)\vec{\mu}_{c_s, v_m}) \\ &\times \mathrm{div}_r\left[\int \mathrm{d}^3 r' \psi_{m's'}(r', r')\frac{\vec{\mu}_{v_{m'}, c_{s'}}}{|r - r'|}\right]. \end{aligned} \tag{7}$$

The analytical part V_{anal} can be written in matrix form as

$$V_{anal}(ms, m's') = (E_X^S - 8\pi/3\mu^2)\begin{pmatrix} 1 & 0 & 0 & 0 \\ 0 & 0 & 0 & 0 \\ 0 & 0 & 0 & 0 \\ 0 & 0 & 0 & 1 \end{pmatrix} \tag{8}$$

with (m, s) and (m', s') in the order, $(\frac{3}{2}, \frac{1}{2})$, $(\frac{3}{2}, -\frac{1}{2})$, $(-\frac{3}{2}, \frac{1}{2})$, and $(-\frac{3}{2}, -\frac{1}{2})$. The definition of the parameters E_X^S and μ can

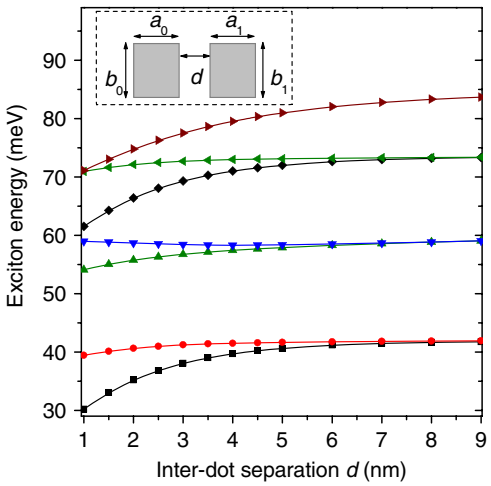

Figure 1. Low-lying exciton levels without the exchange interaction as functions of the interdot separation d for two coupled identical dots with $a_0 = a_1 = 16$ nm and $b_0 = b_1 = 20$ nm. Inset: schematic illustration of a laterally coupled QDM.

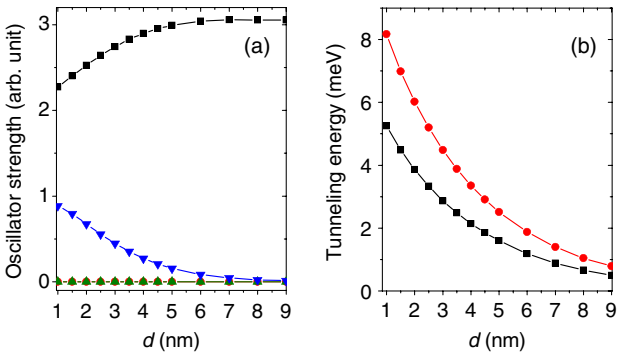

Figure 2. (a) Oscillator strengths of the four lowest exciton states of a QDM in figure 1 (note that the curves of the second and third states are overlapped, and symbols for the corresponding energy levels in figure 1 are used here). (b) Tunnelling energies for the electron (circle) and hole (square), respectively.

be found in [13]. The second term of equation (7), i.e. the nonanalytical term, has a form given by

$$\begin{pmatrix} * & 0 & 0 & * \\ 0 & 0 & 0 & 0 \\ 0 & 0 & 0 & 0 \\ * & 0 & 0 & * \end{pmatrix} \tag{9}$$

where $*$ indicates nonzero matrix elements. In anisotropic QDs, the nondiagonal elements of equation (9) are nonzero, and thus the exciton spin ± 1 states are split into two linearly polarized states. The fine-structure splitting of the doublet is determined by the nondiagonal elements of equation (9).

Similar to the assumption in [12], we use an in-plane anisotropic potential to model a single QD, and the two dots are aligned along the x axis

$$U_{\mathrm{e(h)}} = \nu_{\mathrm{e(h)}}\left[\theta\left(\frac{b_0}{2} - |y_{\mathrm{e(h)}}|\right)\theta\left(\frac{a_0}{2} - \left|x_{\mathrm{e(h)}} + \frac{d+a_0}{2}\right|\right) + \theta\left(\frac{b_1}{2} - |y_{\mathrm{e(h)}}|\right)\theta\left(\frac{a_1}{2} - \left|x_{\mathrm{e(h)}} - \frac{d+a_1}{2}\right|\right)\right] \tag{10}$$

where the two dots with lateral size a_i and b_i for the ith dot are separated by distance d, and ν_{e} (ν_{h}) is the conduction (heavy-hole valence) band offset. The exciton envelope function in QDM can be expanded using the Hermite polynomials as

$$\psi(r_{\mathrm{e}}, r_{\mathrm{h}}) = \sum_{i,j,m,n} C_{ijmn} A_{ijmn} u_i(\alpha x_{\mathrm{e}}) u_j(\alpha y_{\mathrm{e}}) \times \exp\left[-\tfrac{1}{2}\alpha^2(x_{\mathrm{e}}^2 + y_{\mathrm{e}}^2)\right] u_m(\alpha x_{\mathrm{h}}) u_{\mathrm{n}}(\alpha y_{\mathrm{h}}) \times \exp\left[-\tfrac{1}{2}\alpha^2(x_{\mathrm{h}}^2 + y_{\mathrm{h}}^2)\right] \tag{11}$$

where $u_i(x)$ is the Hermite polynomial, A_{ijmn} is the normalization coefficient for the Hermite polynomials, C_{ijmn} is the expansion coefficient and α is a variational parameter. Since we study flat QDs in this paper, the two-dimensional approximation is assumed in the calculation. About 4800 lowest-energy envelope basis sets are taken into account in the diagonalization of the spin-independent matrix H_1 to ensure the convergence of the calculation. We note that the matrix elements of the Coulomb interaction could be obtained analytically [39]. The fine-structure splitting then could be obtained through the perturbation calculation of the exchange interaction V_{ex} since the exchange energy (order of magnitude $\sim\mu$eV) is much less than the exciton level spacings (order of magnitude $\sim$meV). A detailed analysis of the perturbation method is given in the appendix.

3. Numerical calculation and discussion

In QDM, the exciton levels are strongly affected by the tunnelling of the electron and hole as well as the direct Coulomb interaction. The tunnelling energies of the electron and hole in the strong coupling region are much larger than the electron–hole exchange energies. The values of the material parameters used in the calculation are $\nu_{\mathrm{h}} = 81$ meV, $\nu_{\mathrm{e}} = 124$ meV, $m_{\mathrm{e}} = 0.034m_0$, $m_{\mathrm{h}} = 0.053m_0$, $\mu = 6e$ Å, $\epsilon_r = 14$.

3.1. Symmetric quantum dot molecule

In figure 1, low-lying exciton levels without electron–hole exchange interaction for two coupled identical dots with $a_0 = a_1 = 16$ nm and $b_0 = b_1 = 20$ nm are shown as functions of the interdot separation d. At larger d (>8 nm), the coupling between the two dots is very weak and the exciton ground state energy is much closer to that of a single isolated dot with $a = 16$ nm and $b = 20$ nm. As the separation d decreases, the interdot coupling is enhanced and the energy levels are split. Since the quantum confinement and Coulomb correlation are fully taken into account and numerically calculated, the splitting pattern is nonsymmetric and largely distinct from the symmetric splitting pattern of the simple parametric model [36]. We note that the four lowest exciton states are mainly composed of the electron and hole ground state in individual dots. Their oscillator strengths are shown as functions of d in figure 2 (a). As d decreases, the oscillator strength of the ground state decreases while that of the fourth state increases. However, the second and third states

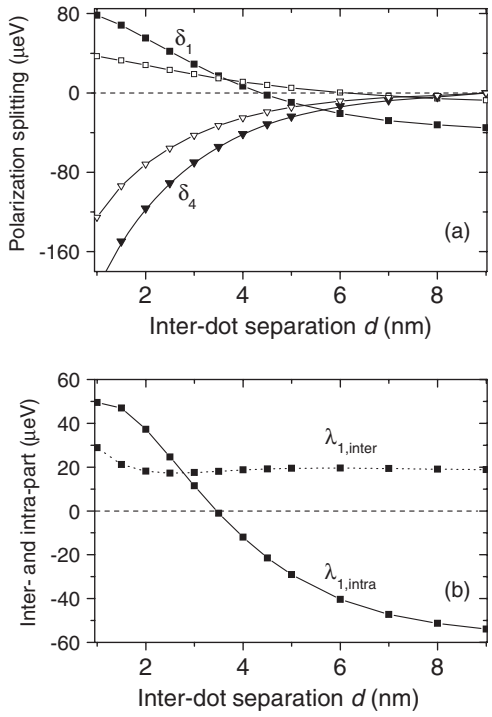

Figure 3. (a) Fine-structure splitting of the exciton ground state with (square) and without (open square) the Coulomb correlation, and of the fourth exciton state with (triangle) and without (open triangle) the Coulomb correlation of QDM in figure 1. (b) $\lambda_{1,\text{intra}}$ and $\lambda_{1,\text{inter}}$ as functions of d.

are always optically inactive. As $d > 7.0$ nm, the oscillator strength of the fourth state becomes negligibly small compared with that of the ground state. In order to better understand the exciton levels, it is helpful to give the electron and hole tunnelling energies $t_{i=e,h} = (E_i^- - E_i^+)/2$ where E_i^+ and E_i^- are energies of single-carrier bonding and antibonding states, respectively. Figure 2(b) shows the tunnelling energies of the electron and hole, which are calculated by the numerical diagonalization of the single-particle Hamiltonian. As d decreases from 9.0 nm to 1.0 nm, the absolute values of the tunnelling energies for the electron (hole) increase from 0.79 meV (0.50 meV) to 8.17 meV (5.25 meV).

Exciton levels of a QDM without the exchange interaction are each four-fold degenerate and the level spacing is around several meV. If the exchange interaction is included, each of the exciton levels is split into fine-structures. One doublet is composed of exciton spin ± 2 states, and the other is composed of exciton spin ± 1 states. For symmetric QDMs in the strong coupling region, the spin ± 1 doublets of the exciton ground and fourth states as shown in figure 1 are optically active and could be observed in the PL and PL-excitation spectra. In figure 3 (a), fine-structure splittings of the exciton ground (δ_1) and fourth states (δ_4) in symmetric QDMs with $a_1 = a_0 = 16$ nm and $b_1 = b_0 = 20$ nm are shown as functions of d. At larger d, the fine-structure splitting δ_1 is negative, e.g. $\delta_1 = -35$ μeV at $d = 9.0$ nm. As d decreases, δ_1 increases from negative values to positive values. At $d \approx 4.4$ nm, δ_1 is zero. However, δ_4 decreases from zero at larger d to -150 μ eV at $d = 1.5$ nm. Although tunnel-coupling induced splitting is negligible at $d = 9.0$ nm as shown in figure 1, fine-structure splitting of the exciton ground state is very different from that of the exciton ground state (-66 μeV) in a single isolated dot of the same size.

According to equations (7) and (9), fine-structure splitting of the exciton ground state can be approximated to first-order as

$$\begin{aligned}\delta_1 &= 2\sum_{r\neq r'_e} \psi_{1,s-m=1}(r,r)\psi_{1,-1}(r',r')V_{\text{ex}} \\ &= \lambda_{1,\text{intra}} + \lambda_{1,\text{inter}}\end{aligned} \tag{12}$$

with

$$\begin{aligned}\lambda_{1,\text{inter}} &= 2\sum_{r\neq r', xx'<0} \psi_{1,1}(r,r)\psi_{1,-1}(r',r')V_{\text{ex}}, \\ \lambda_{1,\text{intra}} &= 2\sum_{r\neq r', xx'>0} \psi_{1,1}(r,r)\psi_{1,-1}(r',r')V_{\text{ex}}.\end{aligned} \tag{13}$$

where $\psi_{i,s-m}(r_e, r_h)$ is the ith exciton eigenfunction of H_1 with exciton spin z component $s-m$, $\lambda_{1,\text{intra}}$ is indeed the long-range exchange interaction within individual dots, and $\lambda_{1,\text{inter}}$ is that between the two dots. Figure 3(b) shows $\lambda_{1,\text{inter}}$ and $\lambda_{1,\text{intra}}$ as functions of d. $\lambda_{1,\text{inter}}$ remains about 20 μeV while $\lambda_{1,\text{intra}}$ is greatly changed from -54 μeV at $d = 9.0$ nm to 50 μeV at $d = 1.0$ nm.

As discussed in section 2, $\psi(r,r)$ is directly related to the calculation of the exchange interaction, and therefore it is important for the study of the variation of fine-structure splitting. In figures 4(a) and (b), $\psi_1(r,r)$ and $\psi_4(r,r)$ are plotted, respectively. $\psi_1(r,r)$ is composed of two s state-like functions in individual dots. For two dots without the tunnel-coupling [40], interdot exchange interaction (i.e. the Förster interaction) is monotonically enhanced as d is reduced. However, if the tunnel-coupling cannot be neglected as shown in figure 4(a), amplitudes of two s state-like functions are reduced at smaller d, which largely compensates the enhancement of $\lambda_{1,\text{inter}}$ at smaller d in the case of neglecting the tunnel-coupling. The consequence is that $\lambda_{1,\text{inter}}$ remains almost constant in the range interdot separations of a few nanometres, as shown in figure 3(b). As d becomes even larger and the tunnel-coupling is negligible, $\lambda_{1,\text{inter}}$ will be proportional to $(d + a_0)^{-3}$ and approach zero as $d \to \infty$. Thus δ_1 will approach the value of a single isolated QD of the same size. Moreover, two s state-like functions are strongly overlapped at smaller d and the anisotropic shape of $\psi_1(r,r)$ in individual dots is largely changed. That is why $\lambda_{1,\text{intra}}$ is greatly varied in the strong coupling region. $\psi_4(r,r)$ is more complicated and there are two nodes along the x axis. Therefore it is meaningless to divide δ_4 into the intra- and interdot exchange interactions. As shown in figure 4(b), $\psi_4(r,r)$ almost disappears at larger d and is largely enhanced at smaller d. The second and third states are always optically inactive. $\psi_2(r,r)$, as shown in figure 4(c) for example, is completely antisymmetric.

The Coulomb correlation between the electron and hole is important for InGaAs QDs with sizes that are comparable to or much larger than the exciton Bohr radius. The exciton envelope function will be greatly changed by the Coulomb correlation and thus the exciton fine-structure splitting could

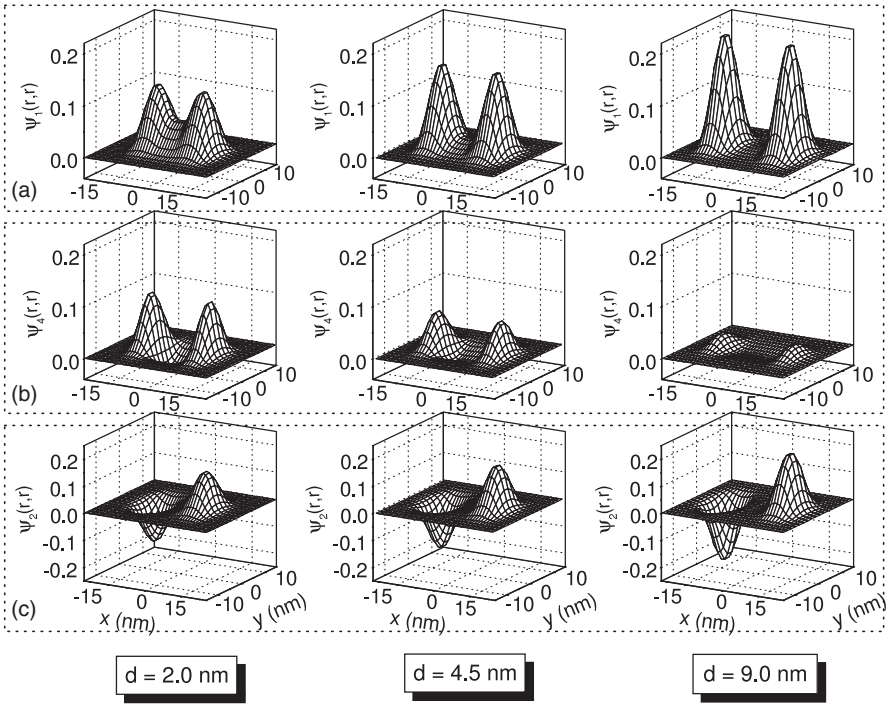

Figure 4. (a) $\psi_1(r, r)$, (b) $\psi_4(r, r)$ and (c) $\psi_2(r, r)$ of QDM in figure 1 for $d = 2.0$, 4.5 and 9.0 nm, respectively.

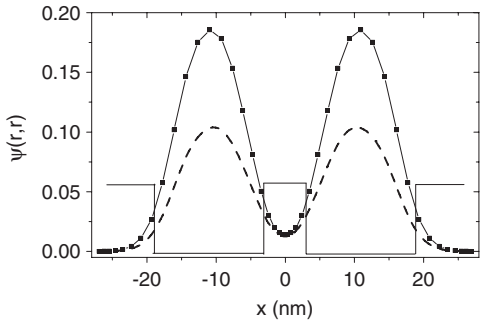

Figure 5. $\psi_1(r, r)$ along the $y = 0$ axis in the QDM of figure 1 at $d = 6.0$ nm with (square) and without (dash line) the Coulomb correlation.

be greatly influenced. Fine-structure splitting of the exciton ground state in a single QD ($a_0 = 16$ nm, $b_0 = 20$ nm) without the Coulomb correlation is -39 μeV, the deviation of which from the value including the Coulomb correlation is as large as 41%. In QDMs, the Coulomb correlation is also very important. Fine-structure splitting of the exciton ground and fourth states without the Coulomb correlation in the same QDM are compared with those that take into account the Coulomb correlation in figure 3. It can be seen that the exciton fine-structure splitting is very different in those with and without the Coulomb correlation. For instance, at $d = 6.0$ nm, $\delta_1 \approx 0$ for the case of an independent electron and hole, while $\delta_1 = -21$ μeV for the case of a correlated electron and hole. $\psi_1(r, r)$ with and without the Coulomb correlation is shown along the $y = 0$ axis in figure 5 for $d = 6.0$ nm, respectively. $\psi_1(r, r)$ in the correlated case is obviously larger than that in the independent one. That is why the exchange interaction and δ_1 are largely changed by the Coulomb correlation in QDMs.

The numerically calculated value of the fine-structure splitting -66 μeV in a single QD with $a = 16$ nm, $b = 20$ nm ($d \to \infty$ limit of QDMs) is consistent with the experimental results of InGaAs QDs with similar sizes [23]. Larger values of the fine-structure splitting might arise from QDs with stronger anisotropy. Although it is now possible to fabricate laterally coupled InGaAs QDs [28], systematic experimental studies of the fine-structure splitting of exciton states in laterally coupled InGaAs QDMs have not yet been reported.

3.2. Nonsymmetric quantum dot molecule

In experimental growth conditions there is size fluctuation in self-assembled quantum dots and it may be difficult to obtain two coupled identical dots. Thus it is important to study the fine-structure splitting in nonsymmetric QDMs. In figure 6(a), the four lowest exciton levels without the exchange interaction for two coupled nonidentical dots with $a_0 = a_1 = 16$ nm, $b_0 = 19$ nm and $b_1 = 20$ nm are shown as functions of the interdot separation d. As $d > 8.0$ nm, the energies of the exciton ground and second states are much closer to the exciton ground state energies of the isolated right and left QDs, respectively. As the separation d decreases, the ground state energy becomes lower. Their oscillator strengths are shown as functions of d in figure 6(b). The oscillator strength of the ground state first increases and then decreases while that of the fourth state increases monotonically as d decreases. In contrast to the identical case, as shown in figure 2(a), the second and third states become optically active. Compared with that of the ground state, the oscillator strength of the third state remains

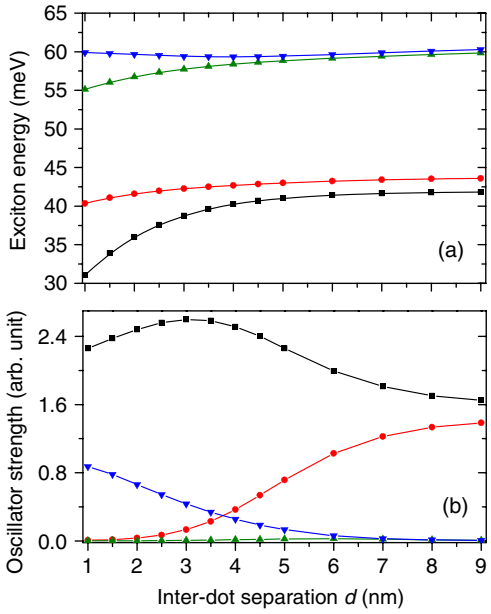

Figure 6. (a) The four lowest exciton levels without the exchange interaction and (b) the corresponding oscillator strengths as functions of d for two coupled nonidentical dots with $a_0 = a_1 = 16$ nm, $b_0 = 19$ nm and $b_1 = 20$ nm.

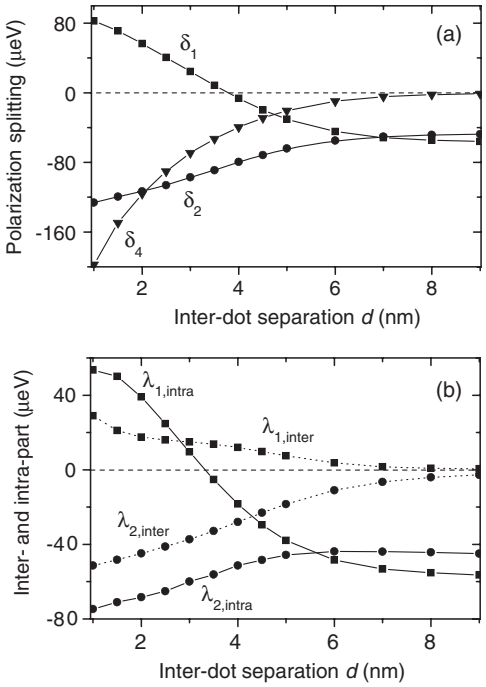

Figure 7. (a) Fine-structure splitting of the ground (square), second (circle) and fourth (triangle) states of QDM in figure 6. (b) $\lambda_{1,\mathrm{intra}}$, $\lambda_{1,\mathrm{inter}}$, $\lambda_{2,\mathrm{intra}}$ and $\lambda_{2,\mathrm{inter}}$ as functions of d.

negligibly small. At larger d, the oscillator strength of the second state is comparable with that of the ground state while it decreases monotonically as d approaches zero.

Fine-structure splittings of three low-lying bright exciton levels are shown as functions of d for the two nonidentical dots in figure 7(a). Similar to the case of two identical dots, δ_1 at larger d is negative, e.g. $\delta_1 = -56$ μeV at $d = 9.0$ nm. As d decreases, δ_1 increases monotonically from negative values to positive values. At $d \approx 3.8$ nm, δ_1 is zero. δ_4 decreases from zero at larger d to -150 μeV at $d = 1.5$ nm. The fine-structure splitting δ_2 of ψ_2 decreases from -48 μeV at $d = 9.0$ nm to -97 μeV at $d = 3.0$ nm. Similar to the definition in equation (13), the inter-and intradot part of δ_2 can also been given. Figure 7(b) shows $\lambda_{1(2),\mathrm{inter}}$ and $\lambda_{1(2),\mathrm{intra}}$ as functions of d. $\lambda_{1,\mathrm{intra}}$ is greatly changed from -56 μeV at $d = 9.0$ nm to 54 μeV at $d = 1.0$ nm. In contrast to the identical case, $\lambda_{1,\mathrm{inter}}$ is zero at $d = 9.0$ nm and is increased as d is reduced. For the second state ψ_2, $\lambda_{2,\mathrm{inter}}$ ($\lambda_{2,\mathrm{intra}}$) is decreased from -3 μeV (-45 μeV) at $d = 9.0$ nm to -37 μeV (-60 μeV) at $d = 3.0$ nm.

In nonidentical cases, $\psi_1(r, r)$ is almost localized in the larger dot at $d = 9.0$ nm as shown in figure 8(a), since the tunnelling energies become much smaller than the orbital energy difference between the two dots. According to equation (13), $\lambda_{1,\mathrm{inter}}$ is proportional to the product of the two s state-like functions in individual dots of $\psi_1(r, r)$. In symmetric QDMs, the two s state-like functions of $\psi_1(r, r)$ approach constants as $d > 9$ nm, and thus $\lambda_{1,\mathrm{inter}}$ of symmetric QDMs will be simply proportional to $(d + a_0)^{-3}$ as $d \to \infty$. However, ψ_1 of nonsymmetric QDMs becomes much more localized in the right QD at larger interdot separations, and, as a result, $\lambda_{1,\mathrm{inter}}$ rapidly decays to zero at larger d in nonsymmetric QDMs as shown in figure 7(b). We note that $\lambda_{1,\mathrm{inter}}$ is different from the Förster interaction in the definition. According to [40], the Förster interaction is defined in the case of negligible tunnel-coupling between the two dots. It is always proportional to R^{-3}, irrespective of the symmetry of two dots, where R is the centre-to-centre distance of the two dots. However, $\lambda_{1,\mathrm{inter}}$ only represents the interdot part of the exchange interaction that contributes to the fine-structure splitting of the ground state, and obviously has that meaning even with tunnel-coupling. We note that in symmetric QDMs at larger d where the tunnel-coupling is negligibly small, $\lambda_{1,\mathrm{inter}}/2$ actually becomes the same as the Förster interaction. In nonsymmetric QDMs at larger d, ψ_1 and ψ_2 are localized in larger and smaller dots, respectively, and the Förster interaction is actually the exchange interaction coupling between ψ_1 and ψ_2 (refer to the appendix).

Similar to the identical case, $\psi_4(r, r)$ has two nodes along the x axis and almost vanishes at larger d, as shown in figure 8(b). $\psi_2(r, r)$ is very localized in the smaller dot at $d = 9.0$ nm as shown in figure 8(c) and therefore $\lambda_{2,\mathrm{inter}}$, similar to $\lambda_{1,\mathrm{inter}}$, also approaches zero at larger d. The values of the functions localized in individual dots of $\psi_2(r, r)$ have opposite signs while those of $\psi_1(r, r)$ have the same sign. Thus, according to equation (13), $\lambda_{1,\mathrm{inter}}$ and $\lambda_{2,\mathrm{inter}}$ have opposite signs, i.e. $\lambda_{1,\mathrm{inter}} > 0$ and $\lambda_{2,\mathrm{inter}} < 0$, as shown in figure 7(b).

4. Summary

We formulate a microscopic theory of exciton fine-structure splitting in laterally coupled QDMs taking into account the

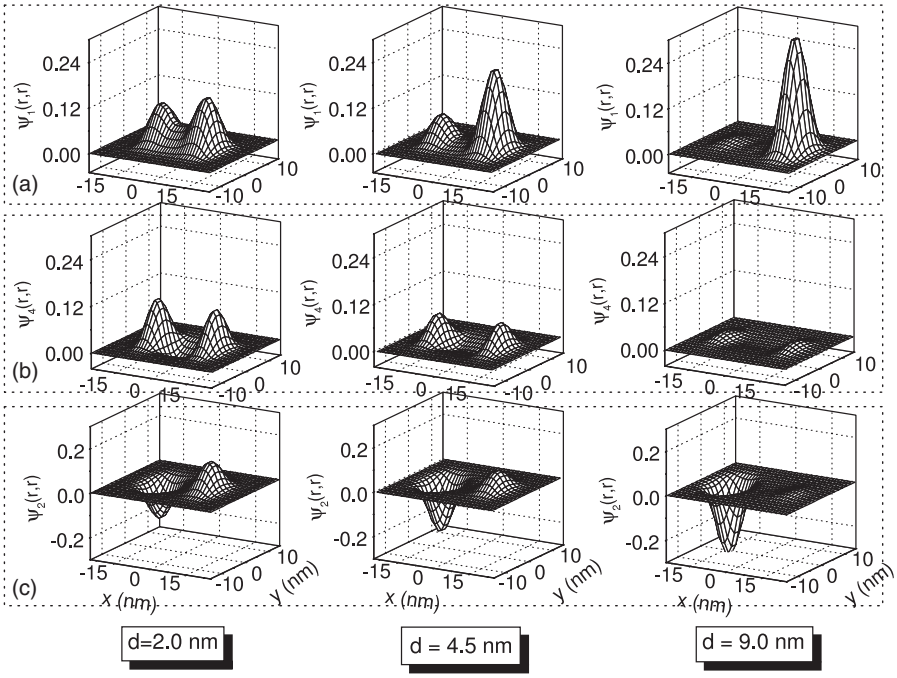

Figure 8. (a) $\psi_1(r, r)$, (b) $\psi_4(r, r)$ and (c) $\psi_2(r, r)$ of QDM in figure 6 for $d = 2.0$, 4.5 and 9.0 nm, respectively.

Coulomb correlation between the electron and hole. We choose the sizes of QDs to resemble those grown in experiments. In typical QDMs, the electron and hole tunnelling energies and the direct Coulomb interaction are essential for the exciton levels and envelope functions. As the interdot separation is reduced, fine-structure splitting of the exciton ground state in QDMs is largely increased while those of the second and fourth states are decreased. At a proper separation, fine-structure splitting of the ground state approaches zero. Fine-structure splittings of the exciton ground and first excited states could be divided into the intra- and interdot exchange interactions, which are sensitive to the tunnel-coupling and symmetry of the QDMs. In symmetric QDMs, the interdot part is almost unchanged in the range of interdot separation of a few nanometres, while in nonsymmetric QDMs the interdot part is rapidly reduced to zero at larger interdot separations. In both symmetric and nonsymmetric cases, the intradot part is greatly varied by the tunnel-coupling, and the fine-structure splitting of the exciton ground state could be varied by about 100 μeV. The fine-structure splitting of the fourth state is greatly enhanced at smaller d while it approaches zero at larger d. In summary, this study provides an efficient way of largely tuning the exciton fine-structure splitting in semiconductor QDs, which is useful and necessary for fine-tuning by the external field.

Acknowledgments

Financial supports from NSF-China (grants no. 10574077 and 10774085), the '863' Programme (no. 2006AA03Z0404) and the MOST Programme (no. 2006CB0L0601) of China are gratefully acknowledged.

Appendix

Using the four lowest eigenstates of H_1 in symmetric QDMs as basis, the matrix representation of $(H_1 + V_{ex})$ is given as

$$\begin{pmatrix}
|\psi_1+1\rangle & |\psi_1-1\rangle & |\psi_2+1\rangle & |\psi_2-1\rangle & |\psi_3+1\rangle \\
E_1+\sigma_{11} & \gamma_{11} & 0 & 0 & 0 \\
\gamma_{11} & E_1+\sigma_{11} & 0 & 0 & 0 \\
0 & 0 & E_2+\sigma_{22} & \gamma_{22} & \sigma_{23} \\
0 & 0 & \gamma_{22} & E_2+\sigma_{22} & \gamma_{23} \\
0 & 0 & \sigma_{23} & \gamma_{23} & E_3+\sigma_{33} \\
0 & 0 & \gamma_{23} & \sigma_{23} & \gamma_{33} \\
\sigma_{14} & \gamma_{14} & 0 & 0 & 0 \\
\gamma_{14} & \sigma_{14} & 0 & 0 & 0
\end{pmatrix}$$

$$\begin{pmatrix}
|\psi_3-1\rangle & |\psi_4+1\rangle & |\psi_4-1\rangle \\
0 & \sigma_{14} & \gamma_{14} \\
0 & \gamma_{14} & \sigma_{14} \\
\gamma_{23} & 0 & 0 \\
\sigma_{23} & 0 & 0 \\
\gamma_{33} & 0 & 0 \\
E_3+\sigma_{33} & 0 & 0 \\
0 & E_4+\sigma_{44} & \gamma_{44} \\
0 & \gamma_{44} & E_4+\sigma_{44}
\end{pmatrix}$$

where the exciton spin ± 2 states are neglected since they are decoupled from the spin ± 1 states, $|\psi_i, \pm 1\rangle$ is the full exciton wavefunction with orbital envelope ψ_i and spin ± 1, E_i is the ith eigenvalue of H_1, $\gamma_{ij} = \langle \psi_i, \pm 1|V_{ex}|\psi_j, \mp 1\rangle$ and $\sigma_{ij} = \langle \psi_i, \pm 1|V_{ex}|\psi_j, \pm 1\rangle$. It should be noted that γ_{ij} is only contributed by the long-range exchange interaction. Moreover, as shown in figure 4, both $\psi_1(r, r)$ and $\psi_4(r, r)$ are symmetric with respect to the $x = 0$ and $y = 0$ axis, while both $\psi_2(r, r)$ and $\psi_3(r, r)$ are symmetric with respect to the $y = 0$ axis but antisymmetric with respect to the $x = 0$ axis. Therefore, according to equations (5) and (7),

the matrix elements $\langle\psi_i, s|V_{ex}|\psi_j, m\rangle$ with (i, j) or $(j, i) = (1, 2)$, $(1, 3)$, $(2, 4)$, and $(3, 4)$ are zero.

Although the fine-structure splitting becomes comparable with the energy splitting without exchange interaction in symmetric QDMs at larger d (e.g. figures 1 and 3(a)), the exchange interaction couplings between ψ_1 and ψ_2 and between ψ_3 and ψ_4 are zero. Moreover, the exchange couplings between ψ_1 and ψ_4 and between ψ_2 and ψ_3 are much smaller than the level spacings $(E_4 - E_1)$ and $(E_3 - E_2)$, respectively. For the nonsymmetric QDMs at larger d, ψ_1 and ψ_2 become localized in separate dots, and thus the exchange coupling between ψ_1 and ψ_2 is actually the Förster interaction, which is less than 10 μeV as $d > 9.0$ nm. The exchange coupling between ψ_3 and ψ_4 rapidly decays to zero at larger d since the amplitude of $\psi_3(r, r)$ and $\psi_4(r, r)$ almost vanishes at larger d as shown in figure 8. However, the level spacings $(E_2 - E_1)$ and $(E_4 - E_3)$ as shown in figure 6(a) approach nonzero constants at larger d (1.77 and 0.44 meV, respectively), which are much larger than the nondiagonal exchange interaction matrix elements. Therefore, all the exchange coupling between two separate levels i and j $(i, j = 1, 2, 3, 4)$ could be neglected, and the fine-structure splitting could be effectively obtained in the first-order approximation in both symmetric and nonsymmetric QDMs.

References

[1] Michler P, Imamoğlu A, Mason M D, Carson P J, Strouse G F and Buratto S K 2000 *Nature* **406** 968
[2] Michler P, Kiraz A, Becher C, Schoenfeld W V, Petroff P M, Zhang L D, Hu E and Imamoğlu A 2000 *Science* **290** 2282
[3] Santori C, Fattal D, Vučković J, Solomon G S and Yamamoto Y 2002 *Nature* **419** 594
[4] Pelton M, Santori C, Vučković J, Zhang B Y, Solomon G S, Plant J and Yamamoto Y 2002 *Phys. Rev. Lett.* **89** 233602
[5] Santori C, Fattal D, Pelton M, Solomon G S and Yamamoto Y 2002 *Phys. Rev.* B **66** 045308
[6] Stevenson R M, Young R J, Atkinson P, Cooper K, Ritchie D A and Shields A J 2006 *Nature* **439** 179
[7] Akopian N, Lindner N H, Poem E, Berlatzky Y, Avron J, Gershoni D, Gerardot B D and Petroff P M 2006 *Phys. Rev. Lett.* **96** 130501
[8] Benson O, Santori C, Pelton M and Yamamoto Y 2000 *Phys. Rev. Lett.* **84** 2513
[9] Gammon D, Snow E S, Shanabrook B V, Katzer D S and Park D 1996 *Phys. Rev. Lett.* **76** 3005
[10] Bayer M, Kuther A, Forchel A, Gorbunov A, Timofee V B, Schäfer F, Reithmaier J P, Reinecke T L and Walck S N 1999 *Phys. Rev. Lett.* **82** 1748
[11] Seguin R, Schliwa A, Rodt S, Potschke K, Pohl U W and Bimberg D 2005 *Phys. Rev. Lett.* **95** 257402
[12] Ivchenko E L 1997 *Phys. Status Solidi* a **164** 487
[13] Takagahara T 2000 *Phys. Rev.* B **62** 16840
[14] Bester G, Nair S and Zunger A 2003 *Phys. Rev.* B **67** 161306(R)
[15] Tartakovskii A I *et al* 2004 *Phys. Rev.* B **70** 193303
[16] Langbein W, Borri P, Woggon U, Stavarache V, Reuter D and Wieck A D 2004 *Phys. Rev.* B **69** 161301(R)
[17] Young R J, Stevenson R M, Shields A J, Atkinson P, Cooper K, Ritchie D A, Groom K M, Tartakovskii A I and Skolnick M S 2005 *Phys. Rev.* B **72** 113305
[18] Greilich A, Schwab M, Berstermann T, Auer T, Oulton R, Yakovlev D R, Bayer M, Stavarache V, Reuter D and Wieck A 2006 *Phys. Rev.* B **73** 045323
[19] Stevenson R M, Young R J, See P, Gevaux D G, Cooper K, Atkinson P, Farrer I, Ritchie D A and Shields A J 2006 *Phys. Rev.* B **73** 033306
[20] Kowalik K, Krebs O, Lemaitre A, Laurent S, Senellart P, Voisin P and Gaj J A 2005 *Appl. Phys. Lett.* **86** 041907
[21] Gerardot B D *et al* 2007 *Appl. Phys. Lett.* **90** 041101
[22] Bayer M, Stern O, Kuther A and Forchel A 2000 *Phys. Rev.* B **61** 7273
[23] Bayer M *et al* 2002 *Phys. Rev.* B **65** 195315
[24] Bayer M, Hawrylak P, Hinzer K, Fafard S, Korkusinski M, Wasilewski Z R, Stern O and Forchel A 2001 *Science* **291** 451
[25] Ortner G *et al* 2005 *Phys. Rev.* B **71** 125335
[26] Gerardot B D, Strauf S, de Dood M J A, Bychkov A M, Badolato A, Hennessy K, Hu E L, Bouwmeester D and Petroff P M 2005 *Phys. Rev. Lett.* **95** 137403
[27] Unold T, Mueller K, Lienau C, Elsaesser T and Wieck A D 2005 *Phys. Rev. Lett.* **94** 137404
[28] Beirne G J, Hermannstädter C, Wang L, Rastelli A, Schmidt O G and Michler P 2006 *Phys. Rev. Lett.* **96** 137401
[29] Ortner G, Bayer M, Larionov A, Timofeev V B, Forchel A, Lyanda-Geller Y B, Reinecke T L, Hawrylak P, Fafard S and Wasilewski Z 2003 *Phys. Rev. Lett.* **90** 086404
[30] Ortner G, Bayer M, Lyanda-Geller Y, Reinecke T L, Kress A, Reithmaier J P and Forchel A 2005 *Phys. Rev. Lett.* **94** 157401
[31] Krenner H J, Sabathil M, Clark E C, Kress A, Schuh D, Bichler M, Abstreiter G and Finley J J 2005 *Phys. Rev. Lett.* **94** 057402
[32] Szafran B, Peeters F M and Bednarek S 2007 *Phys. Rev.* B **75** 115303
[33] Szafran B, Chwiej T, Peeters F M, Bednarek S, Adamowski J and Partoens B 2005 *Phys. Rev.* B **71** 205316
[34] Bester G and Zunger A 2005 *Phys. Rev.* B **72** 165334
[35] Zhu J L, Chu W, Xu D and Dai Z 2005 *Appl. Phys. Lett.* **87** 263113
[36] Bester G, Zunger A and Shumway J 2005 *Phys. Rev.* B **71** 075325
[37] Zhu J L and Xu D 2007 *Appl. Phys. Lett.* **90** 261119
[38] Sheng W D and Hawrylak P 2006 *Phys. Rev.* B **73** 125331
[39] Ugajin R, Suzuki T, Nomoto K and Hase I 1994 *J. Appl. Phys.* **76** 1041
[40] Nazir A, Lovett B W, Barrett S D, Reina J H and Briggs G A D 2005 *Phys. Rev.* B **71** 045334